PHYSICAL REVIEW B VOLUME 17, NUMBER 4 15 FEBRUARY 1978

Electron-spin polarization in low-energy electron diffraction from tungsten (001)

M. Kalisvaart, M. R. O'Neill, T. W. Riddle, F. B. Dunning, and G. K. Walters
Department of Physics, Rice University, Houston, Texas 77001
(Received 4 October 1977)

Combined measurements in low-energy electron diffraction of both electron-spin polarization and intensity are described for beams from W(001). Polarization and intensity are determined in the energy range 20–150 eV for both the 10 and 11 beams at normal incidence and for the 00 beams at angles of incidence from 10° through 18° in 1° steps. Electron-spin polarizations in the range +60%–−80% are observed with polarization values highly dependent on both the energy and the angle of incidence of the primary electron beam. For the 00 beam at 11° angle of incidence and for the 10 beam at normal incidence, comparisons of the present intensity and polarization data with the results of recent theoretical calculations are encouraging with respect to gross features.

I. INTRODUCTION

Extensive comparisons have been made between dynamical model calculations and measured intensities of low-energy electron diffraction (LEED) beams in order to determine the parameters describing a crystal surface.[1] The surface science literature shows that such comparisons have in many cases been rather inconclusive, with the parameters describing even such extensively studied surfaces as tungsten (001) still not very well established.[2] Additional information about the surface, information of value comparable to intensity data, is provided by measurements of the electron-spin polarization of LEED beams. Such polarization measurements can serve as a further stringent test of dynamical LEED models in that any model of the surface that predicts accurately not only the intensity but also the polarization of LEED beams passes a very serious test as to its validity. Furthermore, theory suggests that spin polarization is more sensitive than intensity to certain surface parameters such as the top interlayer spacing and the shape of the surface potential barrier.[3-5]

The physical basis of spin polarization in scattering can most easily be visualized for the case of electron scattering from free atoms of large atomic number.[6] The theoretical results for atomic scattering are in excellent agreement with those of experiment for electron scattering from a variety of atomic targets. The unpolarized incident beam can be considered to consist of equal numbers of electrons with spins "up" and "down" with respect to the scattering plane defined by the incident and outgoing wave vectors. These electrons experience slightly different scattering potentials as a result of a weak spin-orbit interaction. Although this interaction does not affect the direction of the electron spin, it does cause the differential elastic scattering cross sections for electrons with spin up and spin down to be slightly different. As a result, the ratio of up to down electrons present at a particular scattering angle is usually different from unity, giving rise to a net polarization, the sign and magnitude of which will depend on both angle and incident electron energy. If $I\uparrow$ and $I\downarrow$ are the currents of spin "up" and spin "down" electrons, respectively, at a given scattering direction (θ, φ), the polarization $P(\theta, \varphi)$ is defined by $P(\theta, \varphi) = (I\uparrow - I\downarrow)/(I\uparrow + I\downarrow)$, which, for atomic scattering, is always in a direction perpendicular to the scattering plane. Particularly large polarizations occur at angles where one of the two differential scattering cross sections is close to zero, and thus small compared to the other cross section at the same scattering angle. However, since the spin-orbit effect is small, both scattering cross sections have minima at closely spaced angles. As a result, when one cross section is close to zero, the other is small also, so that at scattering angles where large polarizations are realized, the corresponding electron current is at a relative minimum.

In LEED, however, scattering is determined not only by the individual scattering center, which is better represented by a muffin-tin potential rather than by an atomic potential, but also by the multiple scattering occurring in the crystal. Nevertheless, the same spin-orbit effect should cause electrons diffracted from surfaces of crystals of large atomic number to be spin polarized also, with the polarization given by the expression above. Moreover, the data will show that a correlation between high polarization and low intensity carries over to LEED. Because crystal structure has been deduced mainly from the positions of LEED intensity maxima, while polarization tends to emphasize behavior near intensity minima, the two types of measurements should complement one another in

surface structure determinations.[7]

To this end, systematic measurements of both intensity and electron-spin polarization in LEED from a clean tungsten (001) surface have recently been completed.[8] This surface was chosen for study because theoretical LEED polarization calculations have concentrated on it, and because the results of several LEED intensity studies from $W(001)$ are available, enabling direct comparison with the present intensity data.

Polarization and intensity profiles as functions of energy are reported here for the 00, 01, and 11 beams. Profiles are presented for the 00 beam at angles of incidence θ (i.e., the angle between the axis of the electron gun and the normal to the crystal surface) from 10° through 18° in 1° steps. The dependence of the polarization on the azimuthal angle φ (i.e., the angle between the scattering plane and the [01] direction of the two-dimensional surfact net) was obtained for the 00 beam at $\theta = 13°$. Polarization and intensity were also measured for both the 01 and the 11 beams at normal incidence.

Finally, the experimental data are discussed in light of the results of recent theoretical calculations.

II. DESCRIPTION OF EXPERIMENTAL APPARATUS

The experimental apparatus shown in Fig. 1 is contained in two ion-pumped stainless-steel ultrahigh vacuum chambers connected by an accelerating column. The first chamber, with a base pressure of $\sim 2 \times 10^{-10}$ Torr, contains a conventional commercial LEED optics assembly and electron gun. This entire assembly is mounted on a rotary drive and can be turned about a vertical axis through the center of the hemispherical LEED screen. The tungsten crystal is positioned at the center of the LEED optics mounted on a manipulator which allows independent rotation of the crystal about a vertical and a horizontal axis.[9] LEED is performed in the usual manner and the retarding voltage is chosen such that only electrons which have suffered inelastic energy losses of less than 2 eV are present in the LEED beams. The LEED assembly is shielded from stray magnetic fields by use of a mumetal can and from stray electric fields produced by nearby biased components by use of several electrostatic screens. The crystal manipulator, in conjunction with the movable LEED optics, enables any one of several LEED beams to be directed through a narrow horizontal slit cut in the phosphor screen and into the small (2-mm-diam) fixed entrance aperture of a system of electron lenses. The area surrounding this entrance aperture is phosphor-coated to aid in centering the chosen beam on the aperture. Beam intensities are determined by positioning the beam immediately adjacent to the aperture and measuring the light output from the phosphor by use of a spot photometer. The angles reported in this paper have been corrected for this small (<1°) angular adjustment. Electrons entering the lenses through the aperture are focused and directed into the entrance of the accelerating column where they are accelerated to 100 keV. The electrons then enter the second vacuum chamber (base pressure 10^{-8} Torr) where, following further collimation, their spin polarization is determined by the conventional Mott scattering technique.

The Mott scattering technique utilizes the left-right scattering asymmetry produced as a result of spin-orbit coupling when high-energy electrons are elastically scattered at large angles from gold nuclei in a thin gold foil.[6] The scattering asymmetry resulting from this interaction of a gold nucleus and a beam of spin-polarized electrons has been accurately calculated and experimentally verified for a wide range of electron energies and scattering angles.[6] Although multiple scattering of elec-

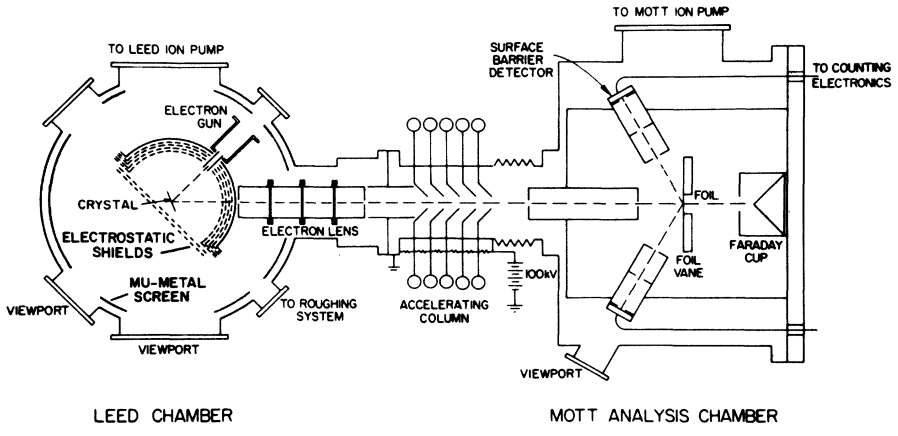

FIG. 1. Schematic diagram of the experimental apparatus.

trons in the fold foil reduces the asymmetry, the correction applicable to the 1000-Å thick gold foils used in this experiment has been determined previously.[10] The asymmetry is largest for electrons scattered in the plane perpendicular to the direction of spin polarization, and, for 100-keV electrons, displays a broad maximum at a scattering angle of 120°. Thus electrons scattered through angles of 120° in the same plane as the LEED scattering plane are counted in two symmetrically placed silicon surface barrier detectors. The pulses produced by these detectors are pulse-height analyzed in two separate channels, one for each detector, and those electrons elastically scattered from the foil are counted on scalers. Using the known scattering asymmetry, the polarization of the electron beam can be deduced from the ratio of counts in the two channels.

It is, however, important to identify the effects of instrumental asymmetries. These are determined by rotating an aluminum foil into the position initially occupied by the gold foil. The aluminum foil exhibits a very small Mott-scattering asymmetry because of its low atomic number.[11] The true gold scattering asymmetry, and hence also the instrumental asymmetry and the electron-spin polarization, may be deduced from consecutive measurements of the counting asymmetries at the gold and aluminum foils. In these measurements, the instrumental asymmetry is typically less than 3%. As a further check of the Mott analysis system, two methods are used to test for the presence of unidentified sources of systematic error in the polarization determinations. First, the polarization of electrons scattered both elastically and inelastically from a deliberately contaminated surface was regularly measured, and zero polarization was observed. Such a result is to be expected for electrons scattered from common surface contaminants of low atomic number (H, C, and O).[12] Second, a tungsten filament is positioned immediately adjacent to the crystal in the LEED chamber. Electrons thermionically emitted from this filament, obviously unpolarized, are directed into the Mott chamber. The polarization of these electrons was always measured to be zero.

Considerable care was exercised in the preparation of the tungsten (001) surface. The crystal was polished to a wafer $\frac{1}{2}\times\frac{1}{4}\times 0.005$ in. oriented $\pm\frac{1}{2}°$ on the (001) face as measured by x-ray diffraction. The polished crystal was electron-beam welded to two tungsten support rods of the manipulator in the LEED chamber. The surface was initially cleaned by resistively heating for tens of hours to 1500 K in research-grade exygen at 10^{-7} Torr, interspersed with "flashings" to 2700 K at 10^{-10} Torr. The temperature of the crystal was measured by use of an infrared telephotometer. Cleanliness of the surface was monitored using the LEED optics in the Auger mode. Extended oxygen treatments were repeated until no carbon could be detected immediately after flashing. During the course of data taking, the crystal was subjected to repeated oxygen treatments consisting of heating the crystal to 1500 K for 3 min in 10^{-7} Torr of oxygen. These treatments were repeated once every two hours. The crystal was flashed to 2700 K prior to each polarization and intensity measurement. Figure 2 shows an Auger scan of the clean crystal surface with no evidence of contamination. A further indication that the flashed surface is indeed reproducibly clean is provided by the excellent repeatability of the measured polarizations and intensities over periods of many months. In addition, as will be discussed later, the intensity-energy (I–V) profiles of this experiment agree well with those reported by other workers.

The data taking was designed to satisfy two requirements. The first requirement is that the instrumental asymmetry of the Mott detector be determined, and the second is that all data be taken soon after flashing the crystal to ensure cleanliness of the tungsten surface. A two-step procedure was adopted. First, the crystal is flashed to 2700 K in vacuum. During the subsequent 3 min, the electrons scattered by the aluminum foil into the two detectors is recorded, with counting rates being typically 50 counts/sec. The gold foil is then rotated into the beam; the crystal is flashed again and for 3 min repeated measurements of the scattering asymmetry from gold are recorded. With the gold counting rate about ten times the aluminum counting rate, gold asymmetries are recorded approximately every 20 sec to give the same number of gold counts as aluminum counts. The short

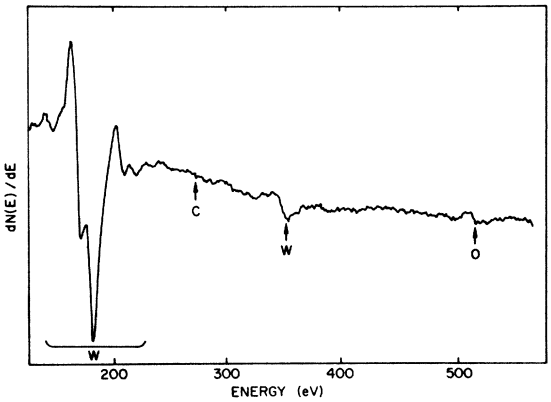

FIG. 2. Auger scan of the clean tungsten surface. Positions of the characteristic tungsten, carbon, and oxygen features are indicated.

data-acquisition time for the gold foil enables any change in polarization with time after flashing to be noted. Although the polarization is in fact observed to be time-dependent, only in exceptional cases discussed later are significant changes observed over the 3 min used for data taking. The temperature of the crystal during the 3 min for which data are recorded was measured and is between 600 and 500 K. Using the known aluminum asymmetry, the polarization is computed for each gold asymmetry. The polarization reported is the mean of the polarizations obtained from all gold asymmetries, with a standard deviation about the mean being typically 2%.

III. EXPERIMENTAL RESULTS AND DISCUSSION

The intensity and polarization of the 00 beam as a function of the incident electron energy are shown in Fig. 3 for angles of incidence θ (i.e., the angle between the axis of the electron gun and the normal to the crystal surface) from 10° through 18° in 1° steps. The primary electron beam is incident along the [01] direction in the tungsten (001) surface. Intensity profiles have been corrected for changes in incident beam current; polarization measurements do not require such a correction. The incidence angles θ can be reproducibly set to better than 0.2°. A systematic offset of $\pm\frac{1}{2}$° may, however, be present at all angles as a result of uncertainties associated with the exact locations of the axes of the electron gun and the Mott analysis system.

In Fig. 4 is shown the dependence of both intensity and polarization on the azimuthal angle of incidence φ for the 00 beam at $\theta = 13$°. It should be noted that the polarization is not necessarily perpendicular to the LEED scattering plane unless this plane is a symmetry plane for the crystal surface. Since the Mott polarization analyzer in this experiment measures only the component of the total polarization perpendicular to the scattering plane, the polarization measured for an arbitrary φ is not necessarily the total polarization. For this reason, the polarizations shown in Fig. 4 for azimuthal angles other than 0° and 45° are the components of the total polarization perpendicular to the scattering plane.

The polarization and intensity of the 10 beam at normal incidence are shown in Fig. 5. The range of energies accessible for study is limited by the geometry of the apparatus. The increased scatter in the measured polarizations results primarily from the requirement that both the crystal and the LEED optics assembly be independently repositioned at each energy.

The polarization and intensity measured for the

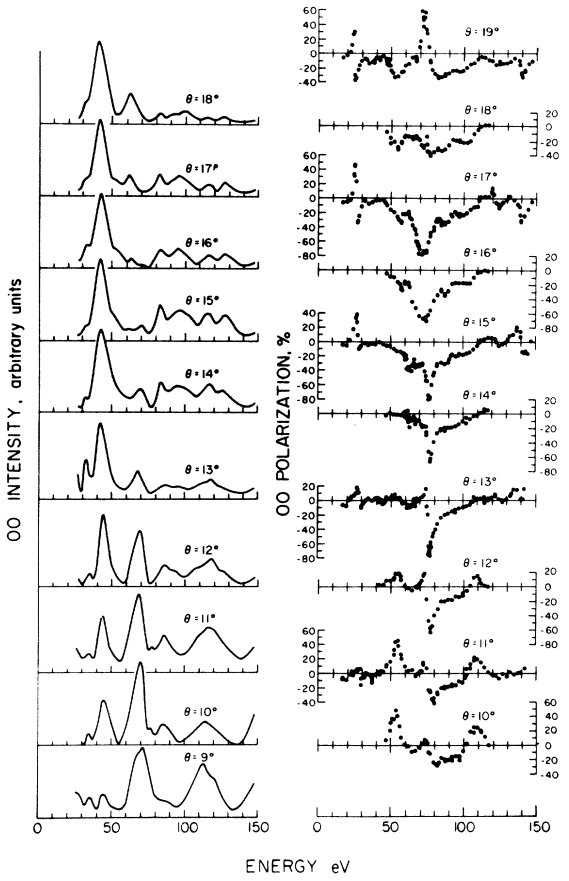

FIG. 3. Measured intensity-energy (I–V) and polarization-energy (P-V) profiles for the 00 beam from W(001) for angles of incidence from $\theta = 10$° through $\theta = 18$°.

11 beam at normal incidence are presented in Fig. 6. Apparatus geometry again limits the energy range.

The present intensity data for all beams are in good agreement with those previously reported. As an example, comparison between the present data and those of other workers[2(a),2(c),13] for the 10 beam at normal incidence is shown in Fig. 7. The close agreement suggests that the present tungsten surface is indeed clean.

It is clear from Fig. 3 that intensity features are not as sensitive to electron energy and angle of incidence as are the polarization features. The sensitivity to electron energy is illustrated by the sharp feature at $E \approx 30$ eV where, at $\theta = 17$°, the polarization changes from +45% to −35% over an energy range of 2 eV; and by the feature at $E \approx 75$ eV where, at $\theta = 13$°, the polarization changes from +20% to −80% over an energy range of 2 eV. The sensitivity of polarization to angle of incidence is shown by the dramatic change in polarization at

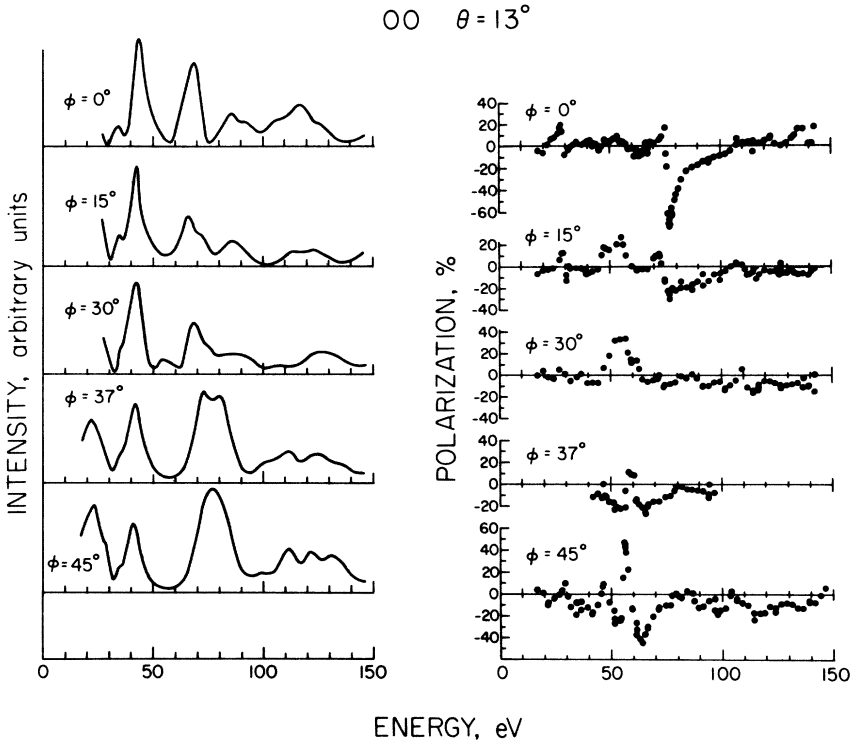

FIG. 4. Azimuthal dependence of intensity and polarization for the 00 beam from W(001) at $\theta = 13°$. The azimuthal angle φ is measured between the [01] direction of the two-dimensional surface net and the scattering plane. The polarization reported is the component of the total polarization perpendicular to the scattering plane.

$E \approx 75$ eV. The large negative polarization peak (−80%) at $\theta = 17°$ becomes a large positive peak (+55%) at $\theta = 19°$.

A direct overlay of intensity and polarization data is shown in Fig. 8 for the 00 beam at $\theta = 11°$. As discussed previously, in atomic scattering large polarizations are observed only at intensity minima. Figure 8 shows that a rough correlation of this kind can also be made in LEED. Note especially the largest polarization features at 55 and 80 eV, where the corresponding intensities are minimum. A related correlation exists between intensity maxima and small polarizations. Examples in Fig. 8 occur at $E = 44$, 68, and 116 eV. However, several obvious exceptions to these correlations are apparent. The polarization peak at

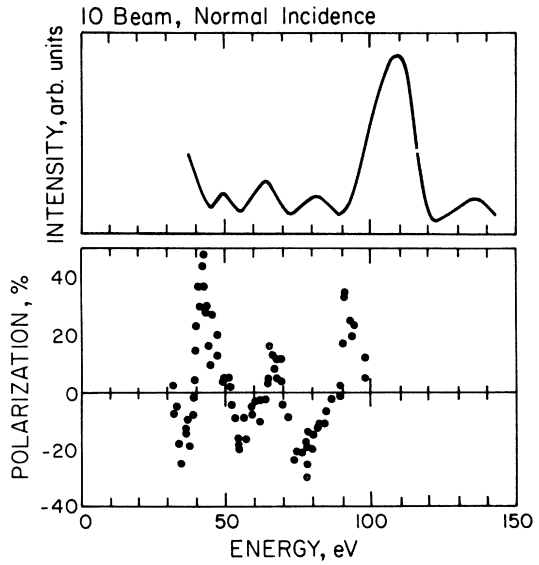

FIG. 5. Measured I–V and P–V profiles for the 10 beam at normal incidence from W(001).

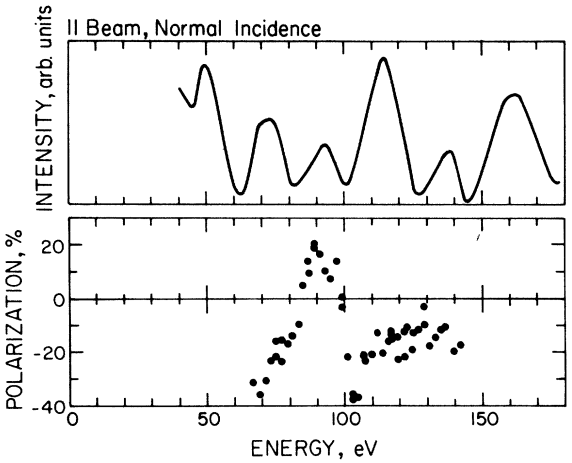

FIG. 6. Measured I–V and P–V profiles for the 11 beam at normal incidence from W(001).

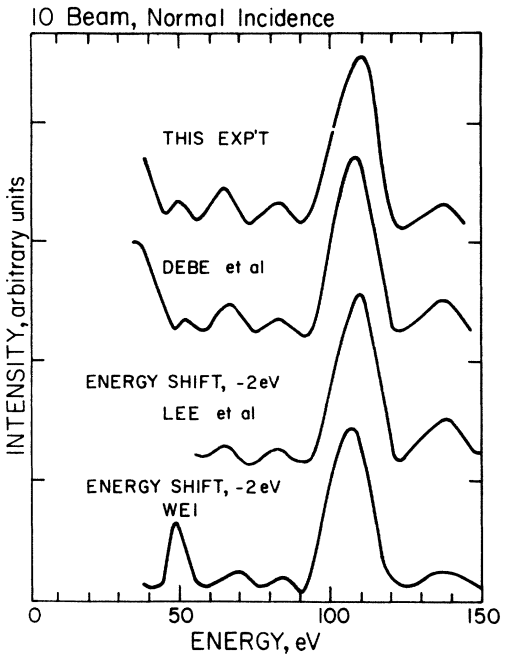

FIG. 7. Comparison of the I–V profiles for the 10 beam at normal incidence from W(001). The curves are from this experiment; from Debe *et al.* [Ref. 2(c)]; from Lee *et al.* [Ref. 2(a)]; and from Wei (1970) (Ref. 13). Note that an energy shift of −2 eV has been applied to the last two profiles.

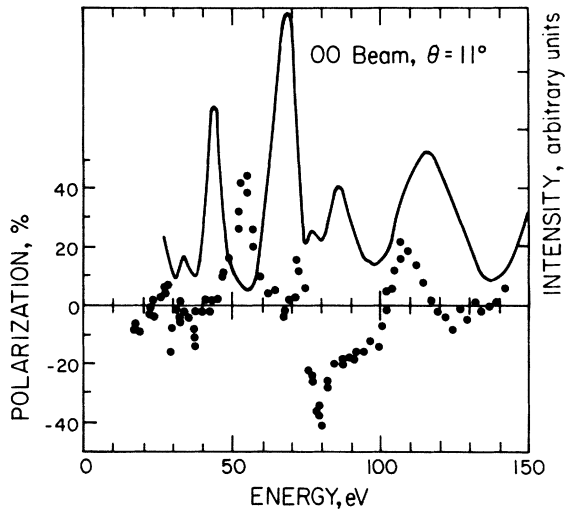

FIG. 8. Comparison of intensity and polarization profiles for the 00 beam at $\theta = 11°$ from W(001).

$E = 107$ eV is not situated at an intensity minimum, and the intensity peak at $E = 85$ eV has a rather large negative polarization associated with it. Detailed study of the correlation of polarization with intensity shows similar effects at all angles of incidence. The very largest polarization features are usually situated on intensity minima, and the largest intensity peaks are usually at energies where polarization is near zero. Exceptions, however, occur and polarizations can have sizable values at energies and angles where intensities are not small. Crystal structure has been deduced mainly from the positions of LEED intensity maxima with little attention given to behavior near intensity minima. The whole energy scale is thus used more effectively if both intensity and polarization measurements are considered in surface analyses.

Both intensity and polarization data have been observed to undergo changes with time after the surface is cleaned. It is because of these changes that all data are taken within 3 min after the crystal is flashed. A study was made of time-dependent changes in intensity profiles for the 00 beam at several angles of incidence. A typical result for an angle of incidence of 11° is shown in Fig. 9. Significant changes are observed with time after flashing, the most prominent being the growth of a peak at $E = 52$ eV and the decay of the peak at $E = 70$ eV.

The major contaminant is probably carbon monoxide coming from the Mott analysis chamber. The Mott chamber cannot be baked because of the presence of sensitive silicon surface barrier detectors and consequently has a base pressure of about 10^{-8} Torr. Conductance into the LEED chamber occurs through the electron lens apertures which direct any impurities exactly at the crystal surface.

Because of the polarization data-taking technique in which a series of about ten gold asymmetries are measured over a period of 3 min, changes in polarization within time periods of 1 min can be detected. For a vast majority (~90%) of the polarization measurements, no variation in polarization

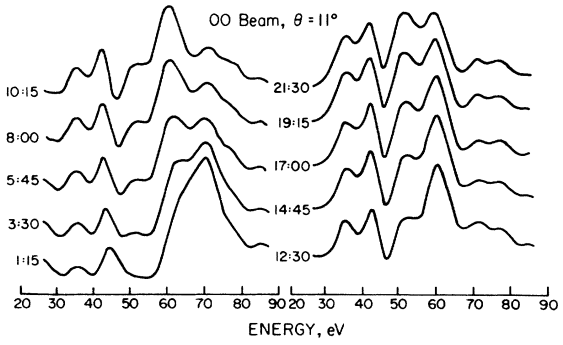

FIG. 9. Repeated I–V curves of the 00 beam from W(001) for $\theta = 11°$. The time in minutes and seconds after flashing the crystal is recorded for each profile.

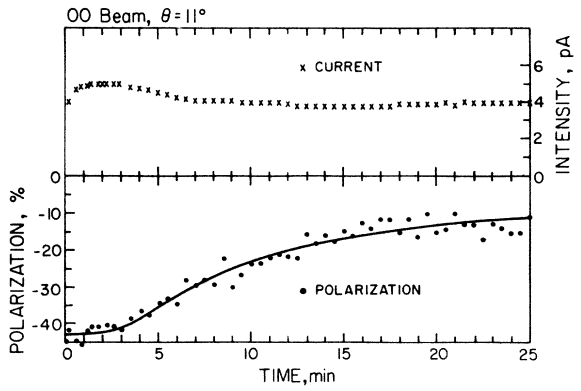

FIG. 10. Polarization as a function of time after flashing the crystal for the 00 beam from W(001) at $\theta = 11°$ and electron energy 79.5 eV. Also shown is the electron current passing through the gold foil and measured by the Faraday cup in the Mott chamber.

is detected during this 3-min period. Over longer periods, the polarization is observed to degrade slowly with time after flashing. A typical example of this degradation is shown in Fig. 10 for the 00 beam of $\theta = 11°$ at an energy of 79.5 eV. The slow drop of polarization toward zero is attributed to adsorption on the crystal surface of layers of contaminants with low atomic number.

At some energies, however, polarizations show a much more marked change with time. An example is shown in Fig. 11 for $E = 54.5$ eV where 3.5 min after the crystal is flashed the polarization has dropped to less than half its original value. At the energy of 54.5 eV, the I–V profile (Fig. 9) shows an intensity minimum. Furthermore, over the same period of 3.5 min, not much change is apparent in the region of this minimum, although a small feature is appearing at $E \approx 52$ eV. Appearances are deceiving, however, as is shown in Fig. 11 by the time-dependence of electron current passing through the gold scattering foil and into

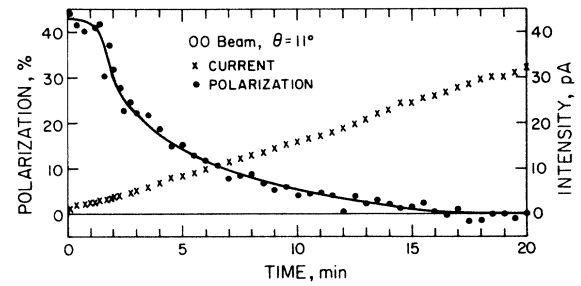

FIG. 11. Polarization as a function of time after flashing the crystal for the 00 beam from W(001) at $\theta = 11°$ and electron energy 54.5 eV. Also shown is the electron current passing through the gold foil and measured by the Faraday cup in the Mott chamber.

the Faraday cup at the back of the Mott chamber. Although the I–V profile does not appear to have changed much at $E = 54.5$ eV, the intensity has in fact increased by a factor of about four in 3.5 min. Thus polarizations can be used effectively to investigate energy regions, primarily intensity minima, where notable changes in intensity are not apparent from I–V curves, although relative intensity changes are in fact quite large. This is a further example of the way in which intensity and polarization measurements complement each other, small changes in I–V profiles being more easily detected and investigated through polarization studies rather than intensity measurements alone.

Preliminary studies of the effects of crystal heating and of depositing controlled adsorbates suggest that the observed time dependences of both polarizations and intensities are determined primarily by surface contamination rather than changes in crystal temperature.[14]

IV. COMPARISON WITH THEORY

Dynamical LEED model calculations incorporating spin have been developed independently by Feder and by Jennings. A recent direct comparison of their calculations showed excellent agreement.[5] Both models are relativistic formulations of the standard nonrelativistic dynamical LEED calculations. Each method solves the LEED problem in three stages.[5] First, the relativistic scattering phase shifts are determined for the muffin-tin potential by numerically solving the radial Dirac equation. Both methods are identical in this respect. The second stage of the calculations, the treatment of intralayer scattering, however, is handled differently in the two formalisms. While Jennings uses a Pauli two-component generalization of the Kambe–Korringa-Kohn-Rostoker method, Feder uses the layer Korringa-Kohn-Rostoker method outlined by Pendry.[1] If N is the number of beams included in the calculation, both methods produce a $4N \times 4N$ transfer matrix for the layer giving the relationship between the $2N$ outgoing plane-wave spinor amplitudes to those incident on the layer. Because of the inclusion of spin, the dimensions of this transfer matrix are twice as large as in nonrelativistic calculations.

The third stage of the LEED problem, interlayer scattering, is also treated differently by Jennings and Feder. Jennings diagonalizes the transfer matrix to obtain the plane-wave spinor amplitudes of the back-scattered waves. Feder, on the other hand, uses the "layer doubling" method.

Since the inclusion of spin doubles the dimensions of the transfer matrices as compared to a

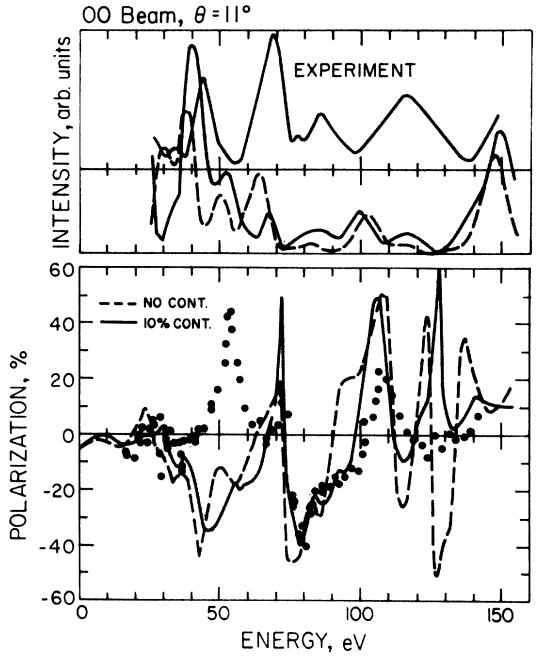

FIG. 12. Comparison of theoretical [Refs. 2(a), 2(c), and 13] and experimental I–V and P–V profiles for the 00 beam from W(001) at $\theta = 11°$. • measured polarizations; — theoretical results, 10% contraction of the top interlayer spacing; -- theoretical results, no surface contraction. An energy shift of −5 eV has been applied to all theoretical profiles.

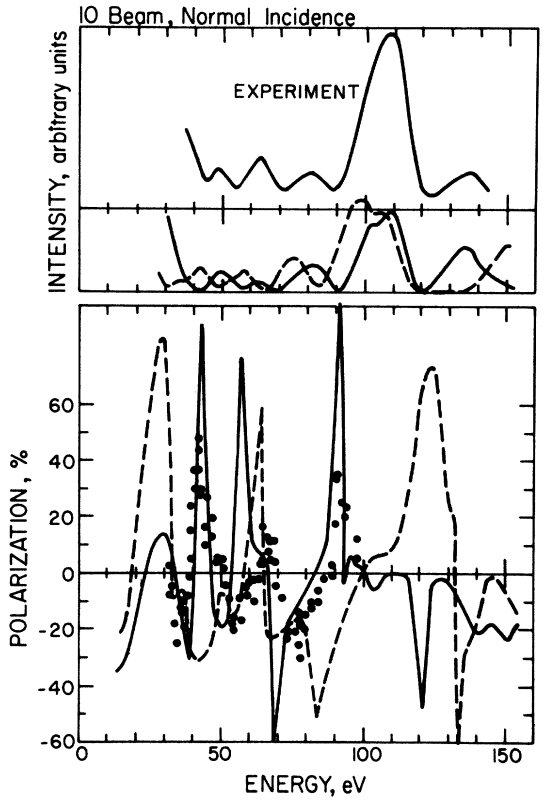

FIG. 13. Comparison of theoretical [Refs. 2(a), 2(c), and 13] and experimental I–V and P–V profiles for the 10 beam from W(001) at normal incident. • measured polarizations; — theoretical results, 10% contraction of the top interlayer spacing; -- theoretical results no surface contraction. An energy shift of −5 eV has been applied to all theoretical profiles.

nonrelativistic calculation applied to the same system, computing time for matrix operations, which scales roughly as n^3 for $n \times n$ matrices, is increased by a factor of about 8 over a nonrelativistic calculation.

Both Feder and Jennings have used their programs to investigate the relative sensitivities of intensity and polarization to various parameters describing a crystal surface.[3,4] These parameters include inelastic processes, top interlayer spacing, and the surface potential barrier. Their calculations suggest that spin polarization is sensitive to these parameters with the sensitivity, in some cases, being greater than for intensity.

Comparisons can be made between intensity and polarization profiles predicted by theory and those measured in this experiment. Figure 12 shows predictions of Feder[15] for the 00 beam with $\theta = 11°$ for two different spacings of the top interlayer, one being the bulk interlayer spacing and the other a 10% contraction. A nonreflecting surface barrier was used in those calculations. Superimposed are the experimentally measured profiles. It is obvious that virtually no agreement exists between the experimental I–V curve and either of the theoretical curves. On the other hand, some agreement exists for polarizations. Both theoretical polarization calculations show the same feature seen experimentally between $E \approx 65$ eV and $E \approx 115$ eV. Although no definite conclusions can be drawn from this energy region, the experimental curve seems to lie closer to the theoretical profile for a surface contracted by 10% than to that for an uncontracted surface. No agreement between theory and experiment, however, exists at either lower or higher energies. This lack of agreement is not surprising considering the poor comparison of intensity profiles.

A second comparison between theory and experiment is shown in Fig. 13 for the 10 beam at normal incidence.[15] The agreement between theoretical and measured profiles is significantly better than for the 00 beam in Fig. 12. Although the double peak at $E \approx 100$ eV calculated theoretically has never been observed experimentally (see Fig. 7), there is reasonable agreement between experi-

ment and theory for a surface 10% contracted.

The polarizations predicted by theory show sharp, large features. Furthermore, in contrast to the intensity results, the calculated polarizations for the two values of top interlayer spacing are completely different. It is on the basis of calculations such as these that Feder[16] suggests that polarization may be more sensitive than intensity to the top interlayer spacing. A comparison of the experimental polarization profile with the theoretical ones shows better agreement for a 10% contraction especially with respect to gross features. However, any conclusion as to this spacing will require theoretical calculations for interlayer spacings on a finer scale.

The rather limited agreement between experiment and theory is perhaps not discouraging, especially considering that the theoretical calculations were made with virtually no experimental polarization measurements to guide the choice of surface parameters.

V. CONCLUSIONS

Simultaneous measurement of intensity and polarization in LEED experiments should provide the basis for improved self-consistency in determination of parameters describing the crystal surface. Crystal structure has previously been deduced mainly from the positions of intensity maxima. In contrast, polarization features are more pronounced near intensity minima. Added confidence should accrue to theoretical structure models capable of predicting both intensity and polarization profiles.

In addition to providing a useful surface diagnostic, polarization in LEED may be useful both as a source of polarized electrons and as a low-energy polarization analyzer. The large measured polarizations suggest that LEED from a crystal surface may provide yet another means for producing spin-polarized electrons.[6] Indeed, in the course of this experiment, and with a 1-μA beam incident on the crystal, polarizations in excess of 70% have been obtained with LEED beam currents estimated to be about 1 nA. The sign of the polarization can be reversed by a judicious change in either the angle of incidence or the energy of the primary beam. Higher currents can easily be obtained at the expense of lower polarizations.

Further, the significant polarization effects in LEED could provide the basis for a spin-polarization analyzer that would operate at low voltages and with greater sensitivity than Mott analysis systems.[14]

ACKNOWLEDGMENTS

The authors are particularly grateful to Professor Thor Rhodin of Cornell University, who provided not only the tungsten crystals used in this study but also encouragement and invaluable counsel regarding the design of the experiment and measurement procedures. We also thank Professor A. Ignatiev and C. Brucker for valuable suggestions and stimulating discussions. This work was supported by Division of Physical Research, U.S. ERDA, and was based on a Ph.D. dissertation by one of us (M.K.), Rice University, 1977. One of us (M.K.) was supported in part by the Fannie and John Hertz Foundation. One of us (F.B.D.) was supported in part by the Alfred P. Sloan Foundation.

---

[1]See, for example, J. P. Pendry, *Low Energy Electron Diffraction* (Academic, New York, 1974).

[2]For example, three recent determinations of the top interlayer spacing of W(001) obtain contractions of (a) 11% [B. W. Lee, A. Ignatiev, S. Y. Tong, and M. VanHove, J. Vac. Sci. Technol. 14, 291 (1977)]; (b) 6% [M. A. VanHove and S. Y. Tong, Surf. Sci. 54, 91 (1976)], and (c) 4.4% [M. K. Debe, D. A. King, and F. S. Marsh, Surf. Sci. (to be published)].

[3]R. Feder, Phys. Status Solidi B 46, K31 (1971); 49, 699 (1972); 56, K43 (1973); 58, K137 (1973); 62, 135 (1974); Surf. Sci. 51, 297 (1975); 63, 283 (1977); Phys. Rev. Lett. 36, 598 (1976).

[4]P. J. Jennings, Surf. Sci. 20, 18 (1970); 26, 509 (1971); 27, 221 (1971); P. J. Jennings and B. K. Sim, Surf. Sci. 33, 1 (1972); P. J. Jennings, Jpn. J. Appl. Phys. Suppl. 2, 661 (1974).

[5]R. Feder, P. J. Jennings, and R. O. Jones, Surf. Sci. 61, 307 (1976).

[6]J. Kessler, *Polarized Electrons* (Springer-Verlag, Berlin, 1976).

[7]For magnetic surfaces, the exchange interaction also can give rise to spin-dependent electron scattering.

[8]See M. R. O'Neill, M. Kalisvaart, F. B. Dunning, and G. K. Walters, Phys. Rev. Lett. 34, 1167 (1975) for a preliminary account of this work.

[9]M. R. O'Neill and F. B. Dunning, Rev. Sci. Instrum. 45, 1611 (1974).

[10]M. McCusker, M.A. thesis (Rice University, 1967) (unpublished).

[11]N. Sherman, Phys. Rev. 103, 1601 (1956).

[12]M. Fink and A. C. Yates, At. Data 1, 385 (1971); M. Fink and J. Ingram, *ibid.* 4, 129 (1972); D. Gregory and M. Fink, At. Data Nucl. Data Tables 14, 3a (1974).

[13]P. S. P. Wei, J. Chem. Phys. 53, 2939 (1970).

[14]D. T. Pierce, R. J. Celotta, and W. N. Unertl, Proceedings of the Seventh International Vacuum Congress and Third International Conference on Solid Surfaces, Vienna, 1977 (unpublished).

[15]R. Feder (unpublished).

[16]R. Feder, Phys. Rev. Lett. 36, 598 (1976).